Table III. Values of Index of Refraction (η), Number Density (ρ), and Molecular Weight (M) of the Siloxane Oligomers

sample	η	ρ (g/cm^3)	M (g/mol)	I (arbitrary units)
A	1.518	0.99	286.5	1.0
B	1.587	1.08	410.7	1.9
C	1.558	1.07	484.8	1.6
D	1.580	1.10	546.9	3.3

respectively). Values of the index of refraction, density, and molecular weight of each oligomer have been determined and are given in Table III. Using these values, we calculated $I = I_{HV}/NL$ for each oligomer. The I values are also given in Table III. The intensity I for oligomer B is nearly twice the intensity of oligomer A, in accord with the number of phenyl rings on the molecule. The 5% discrepancy in the intensity per phenyl group between A and B is insignificant because it is within the experimental uncertainty.

In oligomer C, the two end $CH_3(C_6H_5)_2Si$ units are separated by an intermediate $Si(CH_3)_2$ group, and this results in a decrease in the total intensity in comparison with oligomer B in which the intermediate group is absent. This result suggests that the $Si(CH_3)_2$ group plays a role in affecting the scattering intensity. Consequently, substitution of the methyl group in $Si(CH_3)_2$ with a phenyl ring would result in a higher depolarized Rayleigh intensity in oligomer D. An intensity increase of about 38% more per phenyl group in comparison with dimer B is indeed observed in this oligomer. Thus, the depolarized Rayleigh intensity from the present siloxane oligomer liquids can be satisfactorily related to the intramolecular phenyl group configuration. The intermolecular pair orientational correlation does not directly affect the integrated intensity.

This situation is quite different in the polymer. As shown in Figure 3, as the polymer concentration increases beyond 0.5 g/cm^3, the change in the intensity with the polymer concentration is nonlinear. The intensity data in PPMS suggest the presence of a positive intermolecular pair orientational correlation factor. The positive pair correlation is apparently due to short-range orientational correlation between segments of neighboring chains. However, since the results of oligomers do not indicate the presence of intermolecular pair correlation, it should be of interest to locate the onset point of the intermolecular pair correlation by studying the molecular weight dependence of the Rayleigh scattering intensity of the PPMS oligomer. The result will be useful to correlate the second-order-like transition phenomena with the intermolecular pair orientational correlation function.[17] The effect of intermolecular pair correlation in PPMS on the depolarized Rayleigh spectrum has been discussed in ref 5.

Acknowledgment. This work is supported by the NSF polymer program (Grant No. DMR 82-16221) and chemistry program (Grant No. CHE-83-11088). George Fytas thanks the hospitality of the Department of Chemistry at the University of Utah where a major portion of this work was carried out. We also thank Mrs. I. Brandes of Professor Th. Dorfmuller's laboratory, Universitat Bielefeld, West Germany, for making auxilliary measurements.

Registry No. A, 56-33-7; B, 807-28-3; C, 3982-82-9; D, 3390-61-2.

(17) P. G. de Gennes, *Mol. Cryst. Liq. Cryst.*, **12**, 193 (1971).

^{29}Si Magic Angle Spinning NMR Study on Local Silicon Environments in Amorphous and Crystalline Lithium Silicates

Charles M. Schramm,* B. H. W. S. de Jong,† and Victor E. Parziale‡

Contribution from Occidental Research Corporation, Irvine, California 92713.
Received September 13, 1982

Abstract: ^{29}Si MAS NMR spectra of 12 glasses in the Li_2O–SiO_2 system ($15 < Li_2O < 40$ mol %) have been collected and interpreted in terms of Q_m distribution theory. This theory emphasizes the variation in local silicon environments in silicate glasses. The principal silica species found in the lithium silicate glasses are Q_2, Q_3, and Q_4. Rationalizations are given for the observed metastable liquid immiscibility, viscosity, thermal conductivity, and leaching behavior of amorphous lithium silicates in terms of observed Q_m distributions. Our devitrification experiments indicate that nucleation rates in the Li_2O–SiO_2 system depend on similarities between Q species in glasses and their crystalline analogues. As such the Li_2O–SiO_2 glasses are best described as Porai-Koshits type amorphous solids.

The polymeric structure of silica in amorphous silicates and the degree to which this structure determines the physical and chemical properties of silicate glasses have been a matter of considerable conjecture.[1] Primarily this has been due to the relatively uninformative experimental techniques with which amorphous solids can be probed. There are beyond this experimental barrier some theoretical questions regarding the meaning of structural concepts for amorphous solids.[2]

Recently we have argued on the basis of Si Kβ X-ray emission spectroscopic results on alkali and alkaline earth silicate glasses that the principal structural characteristic of silicate glasses, which is amenable to experimental verification, is the variation in the distribution of local silicon environments.[1] We have designated these distributions Q_m distributions, in analogy to the designation of Engelhardt et al. for silica species distributions in silica containing aqueous solutions.[1,3,4] This Q_m distribution concept, derived from interpretation of X-ray emission spectra, enabled

*Present address: Union Science and Technology Division, Brea, CA 92621.
†Present address: Smitweld BV, 6500 AG Nijmegen, the Netherlands.
‡Present address: Morton Thiokol Inc., Dynachem Corp. Tustin, CA 92680.

(1) A synopsis of most of the salient literature is given in: de Jong, B. H. W. S.; Keefer, K. D.; Brown, G. E.; Taylor, Ch. M. *Geochim. Cosmochim. Acta* **1981**, *45*, 1291-1308.
(2) Philips, J. C. *Phys. Status. Solid B* **1980**, *101*, 473-479.
(3) Engelhardt, G.; Zeigan, D.; Jancke, H.; Hoebbel, D.; Anorg. Z. *Allg. Chem.* **1975**, *418*, 17-28.
(4) Cary, L. W.; de Jong, B. H. W. S.; Dibble, W. E. *Geochim. Cosmochim. Acta* **1982**, *46*, 1317-1320.

0002-7863/84/1506-4396$01.50/0

Table I. Observed Q_m Distributions in Lithium Silicate Glasses

	mol % Li_2O											
species	15.0	17.5	20.0	22.5	24.0	26.0	27.5	30.0	33.0	34.0	37.5	40.0
Q_2	11.9	11.9	12.4	3.9	11.1	7.3	3.6	13.2	21.9	26.8	40.5	57.5
Q_3	37.0	41.1	50.4	63.2	56.6	62.2	66.0	68.9	57.3	62.2	46.0	38.0
Q_4	48.5	47.0	37.2	32.8	29.8	30.5	29.9	16.1	14.6	9.2	12.9	1.8
$Q_0 + Q_1$	2.6	0.0	0.0	0.1	2.5	0.0	0.5	1.8	6.2	1.8	0.6	2.7
Q_4/Q_R[a]	0.94	0.89	0.59	0.49	0.42	0.44	0.43	0.19	0.17	0.10	0.15	0.02

[a] $Q_R = Q_0 + Q_1 + Q_2 + Q_3$ (R = residual).

us to rationalize differences in physical and chemical properties of the alkali and alkaline earth silicate glasses. However, the lack of resolution of the emission spectra prevented an explicit characterization of silicate glasses in terms of silica species distributions.

With the advent of ^{29}Si magic angle spinning NMR spectroscopy (MAS NMR), it has become possible to measure the type and concentration of different local silicon environments in crystalline silicates.[5] In a preliminary report we have demonstrated that amorphous silicates could also be studied by this technique.[6] We shall report here the methods we have developed to extend ^{29}Si MAS NMR to determine the Q_m distribution of noncrystalline silicates.

The system we have chosen for this study is the Li_2O–SiO_2 system, which has an extended glass forming region and which has been used lately as a system on which to test the validity of classical nucleation theory.[7,8] In the following we shall discuss the extent to which Q_m distributions can be determined by ^{29}Si MAS NMR spectroscopy for lithium silicate glasses in the composition region between 15 and 40 mol % Li_2O and how these experimentally determined distributions can be used to rationalize the physical properties, such as viscosity, leachability, and thermal conductivity, of these glasses. We shall finish our discussion with a study of changes in Q_m distribution of two lithium silicate glasses during bulk, i.e., heterogeneous combined with internal, nucleation and growth of crystalline lithium silicates.

Experimental Section

Lithium silicate glasses were prepared from mixtures of reagent grade lithium carbonate and fused silicic acid. The mixtures were heated to 800 °C for 5 h, cooled, ground in an agate mortar under acetone, and heated for 1 h in a Deltech furnace (±2 °C temperature accuracy) at 100 °C above the liquidus temperature for the specific composition. The melts were quenched to room temperature in approximately 15 s. The lithium silicate glasses in the composition region between 17.5 and 30 mol % Li_2O exhibited some opalescence characteristic of the metastable liquid immiscibility prevailing in this composition region. The 15 mol % and 33 and higher mol % Li_2O glasses were clear. Some of the samples were tested for homogeneity on the microprobe scale ($\sim 100\ \mu m^2$), and their silicon concentration was measured. For most samples the compositions quoted represent nominal values.

^{29}Si MAS NMR spectra were collected on a Nicolet NT-200 spectrometer with a 4.7-T wide-bore Oxford magnet. Normal FT-NMR techniques in conjunction with MAS and no decoupling were used to obtain all spectra. An additional capacitor was added to the observe tuning circuit of a ^{13}C CPMAS probe to enable tuning to the ^{29}Si resonance frequency of 39.7 MHz. Both 5-mm and 10-mm i.d. Andrews type rotors were used for collection of the ^{29}Si NMR spectra, with typical spinning speeds of 3 and 2.5 kHz, respectively. A 45° pulse, 30-s recycle delay, 2K data points, and 10-kHz spectral width were used in all cases. Use of increased recycle delays did not affect the spectra, whereas shorter delays resulted in poorer signal-to-noise ratios. Hence, a 30-s recycle delay enables quantitative determination of the Q_m species and is not subjected to errors related to long relaxation times. The ^{29}Si chemical shifts reported in this study are referenced by sample exchange to the chemical shift of benitoite, taken as −93 ppm. The advantage of benitoite as a standard is its narrow line width of 23 Hz (0.6 ppm) and its sensitivity to precise setting of the magic angle (53-Hz line width at 0.5° offset from the magic angle).

Table II. Linear Regression Equations

y	x, mol %	best fit line	regression coeff
% Q_4	15–40	$y = -1.836x + 75.89$	$r = 0.974$
% Q_3	15–30	$y = 2.213x + 2.174$[a]	$r = 0.993$
% Q_3	30–40	$y = -3.089x + 162.3$	$r = 0.971$
% Q_2	15–24	$y = -0.050x + 12.88$[a]	$r = 0.992$
% Q_2	27.5–40	$y = 4.148x - 112.4$	$r = 0.990$

[a] Calculated from data points ignoring the data point at 22.5 mol % Li_2O.

In order to obtain Q_m distributions, we had to resort to curve fitting due to the lack of resolution of the ^{29}Si MAS NMR spectra of glasses. Curve fitting analysis of spectra was carried out by using the NTCCAP program available as part of the NMR software package for the Nicolet 1180 computer. This program allows for the manual, noniterative, analysis of a spectrum composed of overlapping resonances, when values are given for the position, intensity, and full width at half-maximum (fwhm) of the resonances. When the fwhm and intensity for each of the five species present in silicate glass were varied, the error between calculated spectra was minimized. Root mean square errors are calculated with the NCCAP program averaged 7.1 and did not exceed 10.0.

It was found that, upon varying the fwhm, similar values around 600 Hz usually provided the best fit. Use of Lorentzian or mixtures of Lorentzian and Gaussian line shapes resulted in poorer fits than those employing pure Gaussians. Examples of some experimental spectra, calculated spectra, and individual Gaussians from which the calculated spectra were constructed are shown in Figure 1.

Results

^{29}Si MAS NMR spectra of some silicate glasses and the three known crystalline lithium silicates are shown in Figures 1 and 2, respectively. The observed chemical shifts for the local silicon environments in the crystalline phases are −93 ppm (Q_3), −75 ppm (Q_2), and −64 ppm (Q_0). In order to determine if chemical shifts of crystalline substances can be used to interprete ^{29}Si MAS NMR spectra of glasses, values for Q_4 and Q_1 needed to be assigned. For Q_4 the observed chemical shift of quartz was used (−107 ppm), for Q_1 −67 ppm as estimated from a plot of chemical shift vs. connectivity (Figure 3). Application of the chemical shift positions for crystalline materials to glasses did not give proper Q_m distributions.

Values for the mean chemical shifts used by us to fit the spectra of lithium silicate glasses are −107 ppm (Q_4), −92 ppm (Q_3), −82 ppm (Q_2), −69 ppm (Q_1), and −63 ppm (Q_0). The percentages of silica species found by using this fitting procedure are collected in Table I. Analysis of our data by linear as well as nonlinear regression indicates that the linear equations, collected in Table II, describe the species distribution best. The results of this analysis are graphically illustrated in Figure 4 and show that the three major species in lithium silicate glasses between 15 and 40 mol % Li_2O are Q_4, Q_3, and Q_2. The percentage of Q_4 decreases linearly with increasing Li_2O content, that of Q_3 goes through a maximum at 30 mol % Li_2O, and the percentage of Q_2 is approximately constant below 30 mol % Li_2O and increases sharply at higher Li_2O concentrations. The intersection of Q_2 and Q_3 line pairs in Figure 4 occurs at 37.7 mol % Li_2O, and that of Q_2 and Q_4 at 31.5 mol % Li_2O. The estimated accuracy of the concentration of silica species in a glass according to this analysis is around 30%.

The ^{29}Si MAS NMR spectra for 33 and 40 mol % Li_2O containing silicate glasses and their devitrified chemical analogues are shown in Figure 5 and 6. These spectra demonstrate the substantial decrease in line width associated with individual silica

(5) Lipmaa, E.; Magi, M.; Samoson, A.; Engelhardt, G.; Brimmer, A. R. *J. A. Chem. Soc.* **1980**, *102*, 4889–4892.
(6) de Jong, B. H. W. S.; Schramm, Ch. M. *Eos.* **1981**, *62*, 1070.
(7) Rowlands, E. G.; James, P. F. *Phys. Chem. Glasses* **1979**, *20*, 9–14.
(8) Neilson, G. F.; Weinberg, M. C. *J. Non-Cryst. Solids* **1979**, *34*, 137–147.

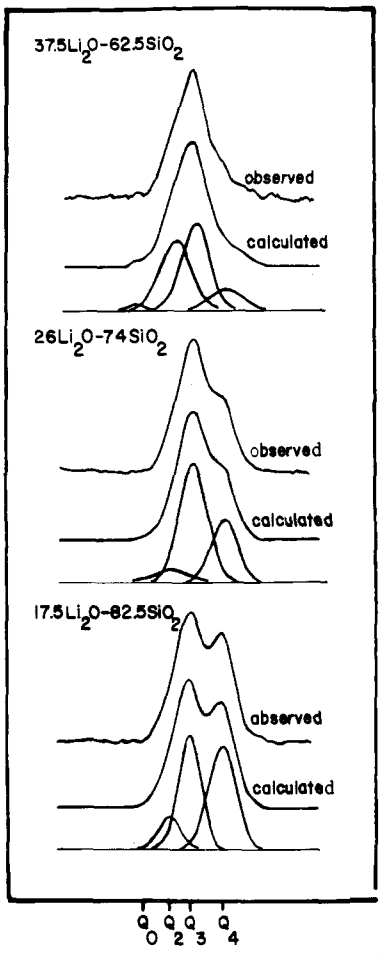

Figure 1. ^{29}Si MAS NMR spectra of three lithium silicate glasses, calculated spectra, and Gaussians used to construct calculated spectra.

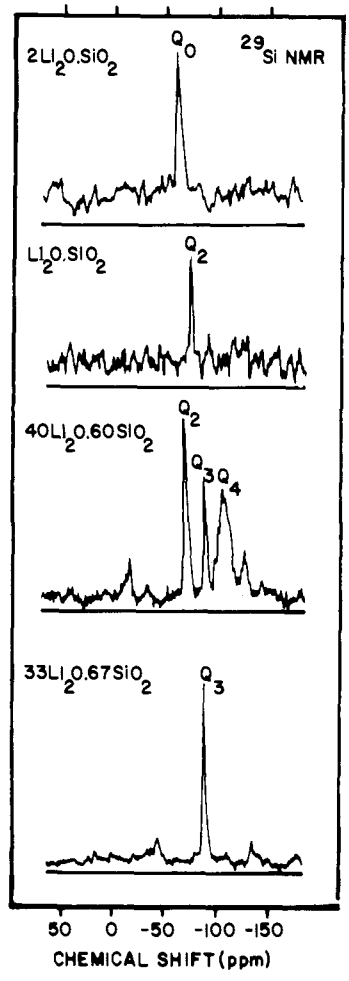

Figure 2. ^{29}Si MAS NMR spectra of the three crystalline lithium silicates and a devitrified lithium silicate glass.

species in crystalline lithium silicates relative to those associated with the silica species distribution in amorphous lithium silicates.

Discussion

Q_m distribution theory is a novel way of describing the structure of silicate glasses.[1,9] It differs from the customary theories because of its emphasis on the local environment around a silicon atom. The need to describe the structure of silicate glasses in terms of Q_m distributions arises from the fact that exactly these local silicon environments are amenable to experimental verification by ^{29}Si MAS NMR spectroscopy.

In order to explain some of the features of the Q_m distribution, we shall start our discussion with this theory. Next we shall discuss possible sources of error in the observed Q_m distribution due to glass preparation and curve fitting procedures, followed by a discussion of the differences in chemical shift between glasses and crystals and of tests for internal consistency of the observed distributions. After rationalizing some physical and chemical properties of lithium silicate glasses in terms of the observed Q_m distributions, we shall finish by discussing the devitrification of two lithium silicate glasses.

A. Q_m Distribution Theory. Before the Q_m distribution theory is described, the tenets of amorphous and crystalline silicates will be pointed out on the basis of the Li_2O–SiO_2 phase diagram and the known crystal chemistry of lithium silicates. Figure 7a shows the phase diagram for the Li_2O–SiO_2 system.[10] Four crystalline silica-containing phases occur in this system, SiO_2, $Li_2O{\cdot}2SiO_2$, $Li_2O{\cdot}SiO_2$, and $2Li_2O{\cdot}SiO_2$. Figure 7b shows the connectivity of these four crystalline phases as a function of Li_2O content. With connectivity is meant the number of Si–O–Si bonds per silica tetrahedron. This number can vary between zero, i.e., no Si–O–Si

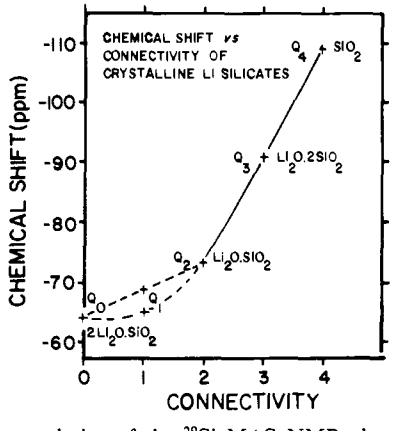

Figure 3. Extrapolation of the ^{29}Si MAS NMR chemical shifts of crystalline lithium silicates to determine the chemical shift of Q_1.

bond per tetrahedron, and four, i.e., four Si–O–Si bonds per tetrahedron. Alternatively stated, the number of bridging oxygens O(br), i.e., oxygens attached to two silicon atoms, can vary between zero and four per tetrahedron. The oxygen atoms in a silicate tetrahedron not attached to two silicon atoms are called nonbridging oxygens (O(nbr)) and represent Si–O–Li linkages (see Figure 8). The existence of a third type of oxygen atoms which might occur in amorphous alkali silicates, free oxygen, O(f), representing Li–O–Li linkages, i.e., oxygen atoms not attached to silicon, has not been verified experimentally to date in the silica-rich part of the Li_2O–SiO_2 system.[11-13]

(9) Keefer, K. D. Ph.D. Thesis, Stanford University, Stanford, CA, 1980.
(10) Kraceck, F. C. *J. Phys. Chem.* **1930**, *34*, 2641–2650.
(11) Brueckner, R.; Chun, H. U.; Goretzkl, H. *Glastech. Ber.* **1976**, *49*, 211–213.

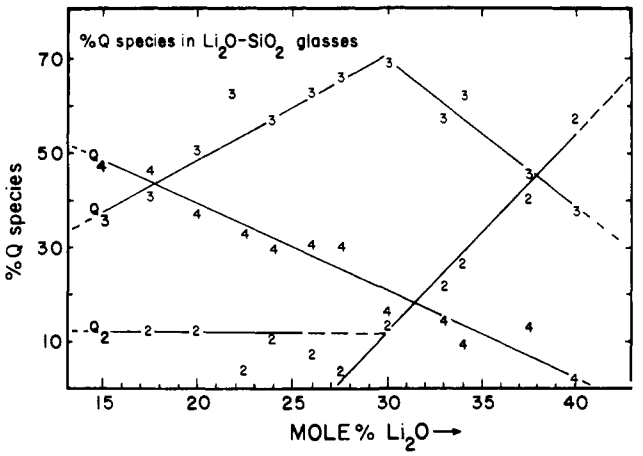

Figure 4. Experimentally determined "best" Q_m distribution in lithium silicate glasses as a function of mol % of Li_2O.

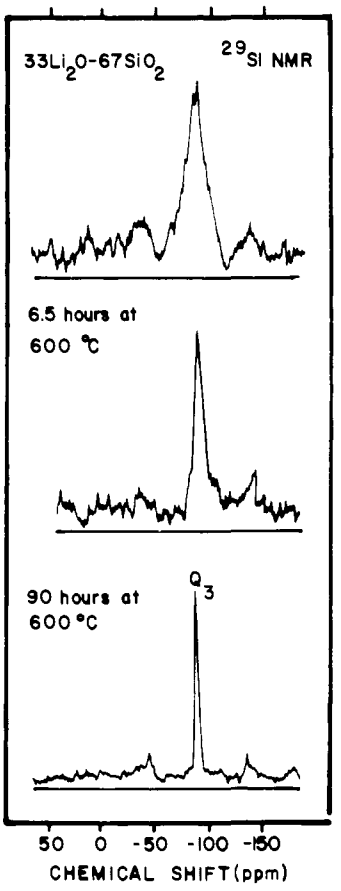

Figure 5. ^{29}Si MAS NMR spectra of $Li_2O{\cdot}2SiO_2$ composition glass before and after devitrification.

Five local silicon environments, defined in Figure 8, are possible in crystalline silicates depending on the number of O(nbr) around the silicon atom in tetrahedral oxygen coordination. These five environments are called Q_0 (all four oxygen atoms around the silicon atom are O(nbr)), Q_1, Q_2, Q_3, and Q_4 (all four oxygen atoms around the silicon atom are O(br)). For example, the local silicon environments in the four silica-containing crystalline phases in the Li_2O–SiO_2 system are Q_4 (SiO_2), Q_3($Li_2O{\cdot}2SiO_2$), Q_2-($Li_2O{\cdot}SiO_2$), and Q_0($2Li_2O{\cdot}SiO_2$), forming, in terms of long-range order of silica tetrahedra, three dimensional networks: corrugated sheets interconnected by lithium atoms in tetrahedral oxygen

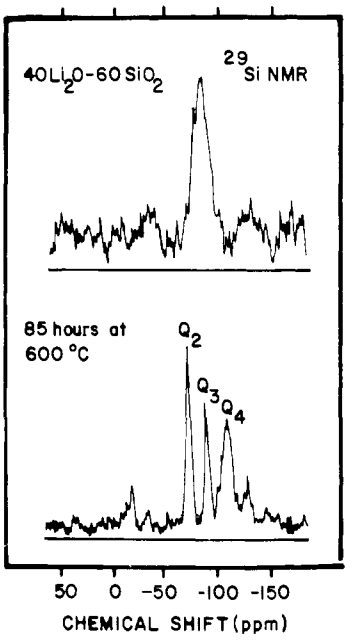

Figure 6. ^{29}Si MAS NMR spectra of $40Li_2O$–$60SiO_2$ composition glass before and after devitrification.

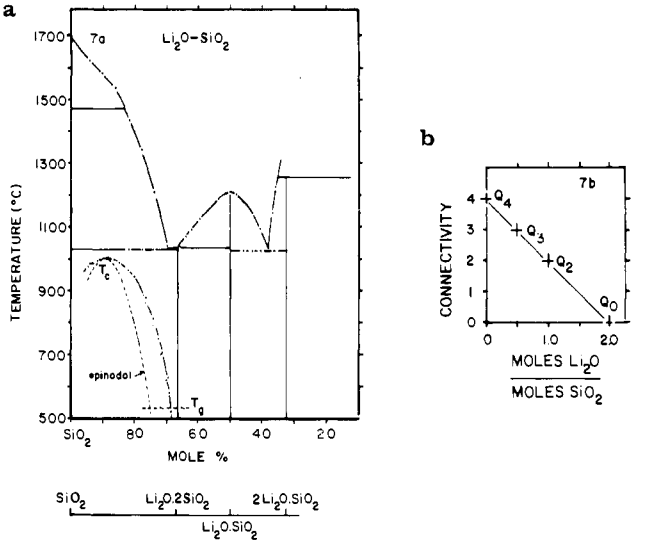

Figure 7. (a) Phase diagram of Li_2O–SiO_2 system and values for the critical temperature T_c.[10,23] T_g is the glass transition temperature. (b) Connectivity of crystalline lithium silicates as a function of Li_2O/SiO_2 molar ratio.

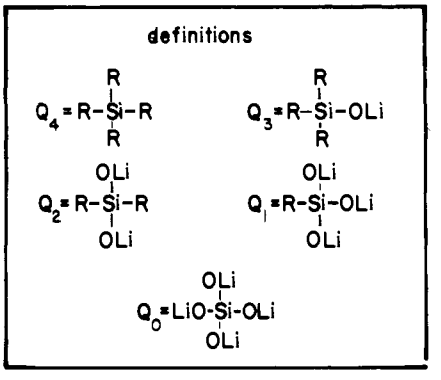

Figure 8. Definitions of the five possible Q species in crystalline and amorphous silicates.

coordination, single chains interconnected by lithium atoms in tetrahedral oxygen coordination, and isolated silicate tetrahedra interconnected by four-, five-, and sixfold oxygen coordinated

(12) Brueckner, R.; Chun, H. U.; Goretzki, H. *Glastech. Ber.* **1978**, *51*, 1–7.

(13) Brueckner, R.; Chun, H. U.; Goretzki, H.; Sammet, M. *J. Non-Cryst. Solids* **1980**, *42*, 49–60.

lithium atoms, respectively.[14-18]

Turning to the Q_m distribution theory, its tenet is that in the absence of long-range order a silicate glass is not characterized by specific local silicon environments, either in a minimally randomized Porai-Koshits solid or in a maximally randomized Zachariassen solid,[2] but rather by a distribution of local silicon environments which may or may not show any resemblance to local environments found in crystalline precipitates from such glass. Thus, instead of discussing the structure of silicate glasses in terms of their crystalline analogues, the Q_m distribution theory seeks a parallel between the silica species distribution in silica-containing aqueous solution and the silica species distribution in silicate glasses.[3,19] When the local silicon environments are counted, the fourth nearest neighbors around each silicon atom are considered. For instance, the local environment around Q_4 may consist of four other Q_4 environments, three Q_4 and one Q_3 environments, four Q_1 environments, etc. The total number of environments possible for each of the five Q species, counted in this manner, are 35, 20, 10, 4, and 1 for Q_4, Q_3, Q_2, Q_1, and Q_0, respectively, in an unconstrained system.[3]

Between the different Q species reaction sequences can be written as shown by Keefer,[9] in which the concentration of O(nbr) is conserved.

$$Li_2O + 2Q_4 = 2Q_3 \quad \text{(depolymerization)} \tag{1}$$

$$2Q_3 = Q_4 + Q_2 \tag{2}$$

$$3Q_3 = 2Q_4 + Q_1 \quad \text{(stepwise condensation)} \tag{3}$$

$$4Q_3 = 3Q_4 + Q_0 \tag{4}$$

Reactions 2, 3, and 4 are devitrification reactions at constant Li_2O content.

An important constraint on the experimentally determined Q_m distribution is that, as long as the ligancy of the lithium atom is assumed to be fixed (one lithium atom per O(nbr)), the number of O(nbr) and O(br) is determined by the stoichiometry of the glass and not affected by variations in the Q_m distribution, or, in other words, the Si/Li_2 molar ratio for a given composition glass has to coincide with that calculated for the observed Q_m distribution. Differences between known and observed Si/Li_2 ratios form the principal means by which to test Q_m distributions as we shall see in the following.

B. Possible Sources of Error in the Q_m Distribution due to Glass Preparation and Curve-Fitting Procedures. The experimentally defined Q_m distribution is quite sensitive to glass preparation procedures, in contrast to most other glass probing techniques. Quench rates have to be fairly well controlled, particularly in systems in which stable or metastable liquid immiscibility occurs. Our samples were selected from triplicate experiments on the basis of minimal visible opalescence of Li_2O–SiO_2 glasses, which have a particular strong tendency to phase separate visibly in the composition region between 17.5 and 27.5 mol % Li_2O.[20]

Beyond the rate of quenching lies the question from which temperature to quench a glass of specific composition. In analogy to the law of corresponding states for gases, we have selected a melting temperature at which the ratio $T_{melting}/T_{critical}$ is approximately constant (~1.50) (see also Kawamoto and Tomozawa[21]). Though our quench rates are fairly low (~100 °C/s) they are fast enough to prevent nucleation and growth in the composition region considered, as judged by the critical cooling rates for glasses in the Li_2O–SiO_2 system (~10 °C/s according to Havermans et al.[22]).

An additional source for chemical inhomogeneity in Li_2O–SiO_2 glasses may be due to spinodal decomposition. This effect may occur when the glass transition temperature, T_g, lies below the critical temperature, T_c. Spinodal decomposition might be operative in the Li_2O–SiO_2 system if one considers as T_g the temperature at which no internal nucleation of $Li_2O{\cdot}2SiO_2$ occurs. The glass transition temperature, thus defined, is 530 °C and hence well below T_c (see Figure 7a).[23-25] As a consequence it is conceivable that a temperature could exist between T_g and T_c, the arresting temperature T_f, at which the state of a glass would be frozen in. The high viscosity of a $Li_2O{\cdot}2SiO_2$ glass at 500 °C (2.5×10^9 P[26]) and the strong increase in viscosity of the alkali–silica systems with increasing silica content make it unlikely that spinodal decomposition is a major contribuant to chemical inhomogeneity in this system.

Crucial for an accurate determination of the Q_m distribution is the line position for each Q species in the distribution. Variations in the mean chemical shift of different Q species are potentially the largest source of error. We shall discuss in the next section how we have attempted to solve this problem.

C. Chemical Shift Differences between Glasses and Crystals and Tests for Internal Consistency of Observed Q_m Distributions. The observed ^{29}Si MAS NMR chemical shifts in our experiments on Li_2O–SiO_2 glasses cover the range of shifts for crystalline silicates, indicating that only silicon atoms in tetrahedral oxygen coordination occur in these glasses.[27]

Initially the observed ^{29}Si MAS NMR spectra for lithium silicate glasses were partitioned according to their various species by using reported chemical shifts of crystalline sodium, potassium, and calcium silicates, augmented with chemical shifts for crystalline silicates from our laboratory.[5,6] The determined distributions proved unsatisfactory, and we attempted next, with similar lack of success, to use chemical shifts of the crystalline lithium silicates as the mean chemical shift around which to construct Gaussian envelopes.

The best results are obtained by using five Gaussians, one for each Q species, at mean chemical shift positions which give the best match between observed and calculated spectra. The two interesting features of this fitting procedure are that the mean chemical shifts for glasses and crystalline lithium silicates approximately coincide with the exception of Q_2 (ΔQ_2 = 7 ppm) and that the fwhm of all Gaussians is identical (~600 Hz). The latter observation is surprising because it might be expected that the fwhm of the Gaussians should vary with the number of possible arrangements of silica species in a glass. The difference in line width between silica species in crystals and glasses (100 vs. 600 Hz) has therefore to be ascribed almost certainly to chemical shift dispersion.

Previously we mentioned unsatisfactory or improper Q_m distributions. The question remains what criteria to use with which to judge these distributions. The minimum requirement for a proper distribution is that calculated and observed spectra coincide with good accuracy. However, a much more important criterion for testing is that the stoichiometry calculated from the observed Q_m distribution is in accordance with the known stoichiometry of the sample.

Table III shows the results of calculating the concentrations of O(br) and O(nbr) as well as the Si/Li_2 ratio for different Q_m distributions. The first four rows show the calculated Q_m distribution which results from the maximum dispersion of lithium

(14) Dollase, W. A. *Z. Kristallogr.* **1965**, *121*, 369–377.
(15) Liebau, F. *Acta Crystallogr.* **1961**, *14*, 389–395.
(16) Voellenkle, H. *Z. Kristallogr.* **1981**, *154*, 77–81.
(17) Liebau, F.; Pallas, I. *Z. Kristallogr.* **1981**, *155*, 139–153.
(18) Tranqui, D.; Shannon, R. D.; Chen, H. Y.; Ijima, S.; Bauer, W. H. *Acta Crystallogr., Sect. B* **1979**, *B35*, 2479–2483.
(19) de Jong, B. H. W. S.; Brown, G. E. *Geochim. Cosmochim. Acta* **1980**, *44*, 1627–1642.
(20) Vogel, W. *Struct. Glass* **1966**, *6*, 114–120.
(21) Kawamoto, Y.; Tomozawa, M. *J. Non-Cryst. Solids* **1981**, *43*, 417–426.
(22) Havermans, A. C. J.; Stein, H. N.; Stevels, J. M. *J. Non-Cryst. Solids* **1970**, *5*, 66–69.
(23) Haller, W.; Blackburn, D. H.; Simmons, J. H. *J. Am. Ceram. Soc.* **1974**, *57*, 120–126.
(24) James, P. F. *Phys. Chem. Glasses* **1974**, *15*, 95–104.
(25) Komppa, V. *Phys. Chem. Glasses* **1979**, *20*, 130–134.
(26) Matusita, K.; Tashiro, M. *J. Non-Cryst. Solids* **1973**, 471–484.
(27) It may be more the exception than the rule that the oxygen coordination in aluminosilicate glass-crystal pairs is similar; see, e.g.: de Jong, B. H. W. S.; Schramm, Ch. M.; Parziale, V. E. *Geochim. Cosmochim. Acta* **1983**, *47*, 1223–1236.

Table III. Comparison between Calculated and Observed Q_m Distributions

Li dispersion	Q_0	Q_1	Q_2	Q_3	Q_4	O(b)	O(nbr)	Si/Li_2[b]	Si/Li_2[c]
maximum									
$17.5Li_2O$–$82.5SiO_2$				42.4	57.6	357.6	42.4	4.71	4.72
$26.0Li_2O$–$74.0SiO_2$				70.3	29.7	329.7	70.3	2.85	2.84
$33.3Li_2O$–$66.7SiO_2$				100.0		300.0	100.0	2.00	2.00
$37.5Li_2O$–$62.5SiO_2$			20.0	80.0		280.0	120.0	1.67	1.67
probable[a]									
$17.5Li_2O$–$82.5SiO_2$		0.4	5.4	30.3	63.9	357.6	42.4		4.73
$26.0Li_2O$–$74.0SiO_2$		1.8	129.6	39.4	46.2	329.7	70.3		2.86
$37.5Li_2O$–$62.5SiO_2$	0.8	7.6	26.5	41.2	24.0	280.0	120.0		1.70
observed									
$17.5Li_2O$–$82.5SiO_2$			11.9	41.1	47.0	335.1	64.9		3.08
$26.0Li_2O$–$74.0SiO_2$			7.3	62.2	30.5	323.2	76.8		2.60
$37.5Li_2O$–$62.5SiO_2$			40.5	46.0	12.9	270.6	129.4		1.57

[a] According to Lacy.[28] [b] Calculated from known stoichiometry. [c] Calculated from Q_m distribution assuming monodentate lithium ligancy.

atoms in lithium silicate glasses, the second three rows the most probable Q_m distribution calculated according to Lacy,[28] and the third three rows show the observed "best" Q_m distribution. Comparison of the Si/Li_2 ratio calculated from the observed "best" distribution with the known Si/Li_2 ratio of the sample shows that the former is off by 35% at the high silica end ($17.5Li_2O$–$82.5SiO_2$) and by 6% at the low silica end ($37.5Li_2$–$62.5SiO_2$). This fairly large fluctuation in error reflects the basic lack in resolution of the ^{29}Si MAS NMR data. A smaller error may be expected in the ratio Q_4/Q_R, in which Q_R consists of $Q_3 + Q_2 + Q_1 + Q_0$, because of the resolved Q_4 peak in the ^{29}Si MAS NMR spectra of the high silica glasses. The Q_4/Q_R ratios, collected in Table I, are quite different from the ones found previously by Si Kβ X-ray emission spectroscopy.[1] Hence variations in line shape of Si Kβ spectral lines in alkali silicate glasses reflect a redistribution of Si 3p states due to various alkalies, rather than differences in Q_m distribution in these glasses.

In summary, our results suggest either that not all possible Q species are equally likely in lithium silicate glasses and hence that the Q_m distribution is constrained in accordance with a Porai-Koshits solid or that different arrangements of one Q species in a glass do not contribute significantly to the NMR signal in contrast to unconstrained Q species in silica-containing aqueous solutions.[3]

D. Q_m Distribution in Lithium Silicate Glasses and Its Relationship to Glass Properties. Inspection of Figure 4 and Table II shows that the dependence of $\%Q_m$ on mol % Li_2O can best be described by linear relationships. The predominant reaction below 30 mol % Li_2O is a depolymerization reaction (reaction 1), as can be shown by using the slopes of the linear regression equations as reaction coefficients:

$$0.92Li_2O + 1.84Q_4 = 2.21Q_3$$

Above 30 mol % Li_2O, the predominant reaction is associated with depolymerization of Q_3 to Q_2. The overall reaction in this composition region is roughly

$$2.65Li_2O + 2.21Q_3 + 3.09Q_3 = 4.15Q_2$$

In the composition region above 30% Li_2O not all Q_4 is first broken down to Q_3, due to attractive interactions between lithium ions in silicate glasses as shown previously.[1] These attractive interactions cause a preferred attachment of lithium ions to those silica tetrahedra which are already connected to one lithium atom, hence accounting for the presence of Q_2 at high silica concentrations in lithium silicate glasses. The high Q_2 concentration may represent the lithium-rich phase in the metastable liquid immiscibility region in the Li_2O–SiO_2 system whereas Q_4 represents the silica-rich region. However, cooperative phenomena, which are not considered by Q_m distribution theory, such as clustering of Q_3 would also account for the metastable liquid immiscibility region. Such Q_3 clustering would be in accordance with thermodynamic considerations of the Li_2O–SiO_2 system.[20]

(28) Lacy, E. D. *Phys. Chem. Glasses* **1967**, *8*, 238–246.

Table IV. Viscosities at 1400 °C of Lithium Silicate Melts and Q_m Distributions of Lithium Silicate Glasses

composition	η, P	Q_2	Q_3	Q_4
$19.9Li_2O$–$80.1SiO_2$	91	12	51	37
$30.0Li_2O$–$70.0SiO_2$	28.2	14	70	16
$33.5Li_2O$–$66.5SiO_2$	19	22	63	15
$35.0Li_2O$–$65.0SiO_2$	13.5	30	59	11

The concentrations of Q_4 and Q_2 become equal around 31.5 mol % Li_2O, at which point metastable liquid immiscibility ceases to occur.[29-31] As shown in Table III, maximum dispersion of lithium atoms in silicate glasses would result in 100% Q_3 and no Q_4 at the $Li_2O{\cdot}2SiO_2$ composition. The fact that fairly large concentrations of Q_4, Q_3, and Q_2 are found at that composition suggests again the existence of attractive lithium–lithium interactions.

Linear extrapolation of the observed Q_m distribution to 0 and 50 mol % Li_2O indicates that at 50 mol % 95% of the Q_m distribution entails Q_2, whereas at 0 mol % 76% entails Q_4. As the ^{29}Si MAS NMR spectrum of fused silicic acid (cristobalite) only shows the presence of Q_4, the slope of the Q_4 line in Figure 4 has to increase with Li_2O concentrations below 15 mol %. The dip in percent Q_2 at 22.5, 26, and 27.5 mol % Li_2O, shown in Figure 4, remains somewhat puzzling but may reflect minor variations in cooling rates of these glasses.

Some physical and chemical properties of lithium silicate melts and glasses can be inferred from the Q_m distribution of the glasses. For instance, the linear decrease in Q_4 with increasing Li_2O content is similar in trend to the nonlinear decrease in viscosity with increasing Li_2O content in lithium silicate melts. The viscosity data for lithium silicate melts at 1400 °C[32] have been collected in Table IV together with the observed Q_m distributions for glasses with similar compositions. From such data partial molar viscosity coefficients can be calculated for each species. These turn out to be 2.8, −0.17, and −0.33 P for Q_4, Q_3, and Q_2, respectively.

Leaching of lithium silicate glasses in the composition region between 20 and 30.3 mol % of Li_2O with HCl increases almost linearly with increasing content.[33] The incongruent dissolution of such glasses suggests that leaching and Q_4 concentration are linearly dependent on one another. This dependence can be expressed by the formula

$$\text{wt \% loss (95 °C, 5 wt \% HCl, 3 h)} = -0.02\ (\%\ Q_4) + 1$$

Similar relations for leaching of lithium silicate glasses with HF have been found by Vogel, who describes the leaching process in

(29) Hautojaervim, P.; Vehanen, A.; Komppa, V.; Pajanne, E. *J. Non-Cryst. Solids* **1978**, *29*, 365–381.
(30) Zanotto, E. D.; Graievich, A. F. *J. Mater. Sci.* **1981**, *16*, 973–982.
(31) Arnold, G. W.; Peercy, P. S. *J. Non-Cryst. Solids* **1980**, *41*, 359–379.
(32) Bockriss, J. O'M.; MacKenzie, J. D.; Kitchener, J. A. *Trans. Faraday Soc.* **1955**, *51*, 1734–1748.
(33) Ahmed, A. A.; El-Batal, H. A.; Ghoneim, N. A.; Khalifa, F. A. *J. Non-Cryst. Solids* **1980**, 57–70.

Table V. Thermal Conductivity of Crystalline Silicates[a]

silica species	conductivity	no. of samples
Q_0, Q_2[b]	10.76 ± 6.03	37
Q_2[c]	9.32 ± 2.56	33
Q_3	7.67 ± 4.47	25
Q_4	4.61 ± 1.37	27

[a] Ki-iti Horai.[39] Units 10^{-3} cal/cm s °C. [b] Q_2 in ring silicates. [c] Q_2 in chain silicates.

terms of the disappearance of Q_3 and Q_2.[20]

The leaching behavior of alkali silicate glasses, i.e., a decrease in leaching with an increase in Q_4 concentration, is similar to that found for crystalline silicates.[34] It is of interest to point out in this context that the point of charge is identical for alkali silicate glasses and quartz (pH ~ 2).[35] Therefore, the silica atoms rather than the alkali atoms are the potential determining atoms of silicate glasses. As the rate of dissolution of quartz is minimal at the point of zero charge,[36,37] it may be expected that the same is true for alkali silicate glasses. It should, however, not be inferred from the above that the surface of quartz and alkali silicate glasses are the same. Dissimilarity in surface characteristics of quartz and alkali silicate glasses can for instance be deduced from the much smaller rate of silica dissolution of quartz as well as from the adsorption isotherms of alkali silicate glasses which show that the amount of water adsorbed as a function of relative humidity depends on the Q_4 concentration in the glass.[1,38]

Rationalization of the thermal conductivity of glasses forms another application of Q_m distribution theory to the physical and chemical properties of glasses. Thermal conductivity of amorphous materials is of importance in catalyst design because local heating, for instance in oxidation catalysis, has to be prevented. The average thermal conductivity data for crystalline silicates, collected in Table V, show a decrease with increased branching of the silica species.[39] It may therefore be expected that amorphous silicate supports with higher concentrations of Q_2, Q_1, or Q_0 will conduct heat better. Hence lithium silicate glasses with higher Li_2O content will be considerably better heat conductors than those with lower Li_2O content. On the other hand, the stability of an alkali silicate glass decreases with increasing O(nbr) content as shown above.[40] Therefore, in applications of this nature an optimal Q_m distribution has to be sought, which maximizes the thermal conductivity as well as the stability of an amorphous silicate.

E. Devitrification of Lithium Silicate Glasses. The maximal rate of internal nucleation of $Li_2O{\cdot}2SiO_2$ composition glasses occurs at a temperature around 480 °C.[8] By keeping a $Li_2O{\cdot}2SiO_2$ composition glass for varying lengths of time at this temperature an isochemical crystalline precipitate is formed with as silica species corrugated two-dimensional sheets of Q_3. The predominant questions in nucleation theory focus on the rate determining step in the devitrification process, one of the hypotheses postulating that this rate determining step depends primarily on a structural relation between glass and precipitate from such a glass.[1,41-43] We have studied the $Li_2O{\cdot}2SiO_2$ glass-crystal pair in order to test this hypothesis.

Inspection of Figure 4, which shows the "best" Q_m distributions to date, shows that the most important species in a $Li_2O{\cdot}2SiO_2$ glass is Q_3. Moreover the mean chemical shift of Q_3 in the lithium silicate glasses, −92 ppm, is similar to the one observed in crystalline $Li_2O{\cdot}2SiO_2$, −93 ppm. This similarity in chemical shift of Q_3 between glass-crystal pairs suggests that the local silicon environments in both phases are similar to one another. We conclude from these results that the most likely description of the structure of a $Li_2O{\cdot}2SiO_2$ glass invokes the existence of a micellar arrangement similar to the one encountered in its crystalline analogue. That it is possible at all to make a $Li_2O{\cdot}2SiO_2$ composition glass has to be ascribed to the relatively high concentration of Q_2 and Q_4 (see Table I), which are incompatible with the local environments present in crystalline $Li_2O{\cdot}2SiO_2$.

One last question we want to answer is what happens during devitrification of a lithium silicate glass at compositions between the two crystalline phases $Li_2O{\cdot}2SiO_2$ and $Li_2O{\cdot}SiO_2$. A $40Li_2O{\cdot}60SiO_2$ glass should devitrify according to the Li_2O–SiO_2 phase diagram (Figure 7a) with precipitation of $Li_2O{\cdot}2SiO_2$ and $Li_2O{\cdot}SiO_2$. Our ^{29}Si MAS NMR spectrum, shown in Figure 6, shows that this is the case. However, during devitrification, the concentration of Q_4 increases. We interprete this increase as being due to one of the devitrification reactions in which Q_3 is broken down to Q_4 and Q_2 according to reaction 2. This is the first, and up to this time only, devitrification experiment in which we have found evidence for a stepwise condensation reaction.

Li_2O–SiO_2 composition glasses with Li_2O concentration above 40 mol % cannot be quenched by normal quench techniques due to a high concentration of Q_2. Comparison of the Q_3 species concentration in $33.3Li_2O$–$66.7SiO_2$ and the Q_2 concentration in $40Li_2O$–$60SiO_2$ glass suggests that, if roughly 60% of the Q species present in the glass is the same as that found in the precipitate from such a glass, no glass formation is possible any longer. This is apparently true even if the specific Q environments exhibit quite different arrangements as suggested by the large chemical shift difference (7 ppm) between Q_2 in lithium silicate glasses and crystalline $Li_2O{\cdot}SiO_2$.

Our conclusion from these ^{29}Si MAS NMR experiments on lithium silicate glasses is that the Q_m distribution in lithium silicate glasses is constrained. That therefore this particular glass system is best described as a Porai-Koshits rather than a Zachariassen solid. Our experiments on glasses reported elsewhere also indicate that not every silicate glass can be considered a Porai-Koshits solid but that different silicate glasses exhibit the range between Porai-Koshits and Zachariassen solids, especially in the presence of "randomizers" such as aluminum.[44,45]

Summary and Conclusions

^{29}Si MAS NMR spectra of lithium silicate glasses have been interpreted with Q_m distribution theory, which emphasizes the characterization of the structure of silicate glasses in terms of their local silicon environments. The predominant local silicon environments in Li_2O–SiO_2 glasses (15–40 mol % Li_2O) consist of Q_2, Q_3, and Q_4. Metastable liquid immiscibility in the composition region between 17 and 30 mol % Li_2O may be due to the presence of Q_2 at low Li_2O concentrations but can also be ascribed to a cooperative arrangement of Q_3.

Viscosity of melts, leaching of glasses in aqueous solutions, and thermal conductivity of glasses are governed by the concentration of Q_4. Bulk nucleation of lithium silicate glasses is predetermined by the specific species concentration for a particular composition. Our results indicate that glasses in the Li_2O–SiO_2 system nucleate faster if local silicon environments in the glass, compatible with those in the crystalline precipitate, are present in sufficient concentration. All evidence collected indicates that the structure of lithium silicate glasses should be described in terms of a minimally randomized Porai-Koshits solid rather than a maximally randomized Zachariassen solid.

Registry No. SiO_2, 7631-86-9; Li_2O, 12057-24-8; ^{29}Si, 14304-87-1; lithium silicate, 12627-14-4.

(34) Terry, B. Hydrometallurgy **1983**, *10*, 135–150.
(35) Horn, J. M.; Onoda, G. Y. *J. Am. Ceram. Soc.* **1978**, *61*, 523–527.
(36) Kamiya, H.; Shimokata, K. *Proc. Int. Symp. Water–Rock Interact.* **1974**, *1*, 1.
(37) Dibble, W. E. Thesis Stanford University, Stanford, CA 1980.
(38) Zhdanov, S. P.; Yastrebova, L. S.; Koromal'di, E. V.; Khvoschchev, S. S. *Struct. Glass* **1966**, *6*, 135–138.
(39) Horai, K. *J. Geophys. Res.* **1971**, 1278–1308.
(40) Duffy, J. A.; Ingram, M. D. *J. Non-Cryst. Solids* **1976**, 273–278.
(41) Tomozawa, M. *Phys. Chem. Glasses* **1972**, *13*, 161–166.
(42) Fratello, V. J.; Hays, J. F.; Spaepen, F.; Turnbull, D. *J. Appl. Phys.* **1980**, *151*, 6160–6164.
(43) Fenn, P. M. *Can. Mineral.* **1977**, *15*, 135–161.
(44) de Jong, B. H. W. S.; Schramm, Ch. M.; Parziale, V. E. *Geochim. Cosmochim. Acta*, in press.
(45) Philips, J. C. *Solid State Commun.* **1983**, *47*, 203–206.